

## A Simple Method for Extracting the Natural Beauty of Hair

Ken-ichi Anjyo\*† Yoshiaki Usami\* Tsuneya Kurihara†

Hitachi, Ltd.

### ABSTRACT

A simple differential equation method is proposed for modeling the aesthetic features of human hair. In the method, a simplified cantilever beam simulation is employed for hairstyle modeling, which allows hairdressing variations with volumetric and realistic appearance. In order to describe the dynamical behavior of hair in an animation, one-dimensional projective differential equations of angular momenta for linked rigid sticks are also derived. For the problem of collision detection between hair and a human head, the "rough" approximate solution is provided, which gives visually satisfactory results by solving the projective equations under a pseudo-force field. The hair's pliability can be controlled by using a set of stiffness parameters in the method. In addition, a fast rendering technique for anisotropic reflection is introduced, which is derived from Blinn's specular model. The efficiency of the proposed method is illustrated by the still images and short animations obtained.

**CR Categories and Subject Descriptors:** I.3.3 [Computer Graphics]: Picture/Image Generation; I.3.7 [Computer Graphics]: Three-dimensional Graphics and Realism.

**General Terms:** Algorithms, Graphics

**Additional Keywords and Phrases:** human modeling, hair, differential equation, simulation, collision detection, anisotropic reflection

### 1. Introduction

Modeling human characters is one of today's most challenging issues in computer graphics [6]. In particular realistic representation of human hair presents many problems to overcome, which appear in all aspects of computer graphics technologies, i.e. rendering, shape modeling and animation.

In the late 1980's several new techniques appeared relating to synthetic hair representation, but most of them were only for rendering furry objects, such as a teddy bear [4] or spider [7], rather than human hair. More recent works [5, 8] have shown that naturalistic human hair rendering can also be performed as variations of previous research, including the above techniques. These successful results for rendering have led us to achieve more realistic syntheses of human characters, along with the development of modeling and animation techniques. However research for hairstyle modeling or for describing dynamical behavior of hair is not completed yet.

In an actual hairstyling process, many artificial techniques are provided by a hairdresser, such as shearing, perming, and combing. These may be very important factors in selecting a desirable hairstyle. Other essential factors lie in the natural and physical properties of hair, which include hair color, width, pliability and volumetric appearance. Therefore a hairstyle modeling method for our purpose should be computationally tractable, while considering these two aspects of actual hairstyling: artificial and intrinsic factors. A previous work [11] proposed models for describing some artificial factors. The intrinsic factors may be achieved partly by the rendering techniques mentioned above. However, for *shape* modeling of hair, a novel technique dealing with the intrinsic factors as well as the artificialities is desired.

In order to model the dynamical behavior of hair in an animation, a physically based modeling approach [9] may not be applicable. In a physically meaningful simulation, the number of unknown functions appearing in the derived differential equations must be too large to obtain satisfactory results at reasonable computational cost. In particular it is impossible to numerically treat self-interaction or collision detection of a large amount of hair, typically tens of thousands of hairs. On the other hand, supposing several simplifications, such as disregard for inter-hair collision, a variation on the philosophies of physically based modeling has been recently proposed [8]. In any case physically faithful dynamics of hair

\* Hitachi Research Laboratory, 4026 Kuji, Hitachi, Ibaraki 319-12

† Hitachi Central Research Laboratory, 1-280 Higashi-Koigakubo, Kokubunji, Tokyo 185

‡ Current address: Systems Engineering Division, Hitachi, Ltd., 4-6 Kanda-Surugadai, Chiyoda Tokyo 101

Permission to copy without fee all or part of this material is granted provided that the copies are not made or distributed for direct commercial advantage, the ACM copyright notice and the title of the publication and its date appear, and notice is given that copying is by permission of the Association for Computing Machinery. To copy otherwise, or to republish, requires a fee and/or specific permission.

can be considered to reflect an aspect of the hair's beauty, so that a differential equation approach would not be avoided. Consequently the differential equation approach for our purpose should employ easy-to-solve equations which still hold some aesthetics of hair as the physically faithful realities.

This paper is therefore intended to provide a step forward in modeling the aesthetic features of human hair, focusing on hairstyling and dynamics. However, we do not emphasize the rigorous physics necessary for modeling. The heart of the proposed method lies in deriving simple differential equations as the *visual analogies*, while abandoning a physically rigorous formulation or its simplification [9, 8]. This allows the method to employ several simple and intuitive ideas for fast processing while preserving a visually satisfactory reality.

The organization of the paper is as follows: In section 2 we describe the hairstyle modeling technique, which employs a simple ordinary differential equation governing cantilever beam deformation. The obtained hairstyle variations illustrate the efficiency of the proposed technique. In section 3, we introduce simple differential equations of one-dimensional angular momenta for describing dynamical behavior of hair. Collision detection or avoidance of hair strands is then discussed. The animation examples are also shown. In section 4 the rasterization process in our method is briefly presented. The computational costs are also discussed along with the examples obtained. In addition a fast rendering method for representing anisotropic reflection of hair is derived. Concluding remarks are made and further work is discussed in section 5.

## 2. Hairstyle modeling

In our case a geometrical model of a human head with texture is obtained from the three-dimensional digitized data of an actual mannequin, whereas the textures of such items as eyes, mouth, and teeth are made by a designer using interactive operations. The hairstyle modeling then consists of the following steps:

- [ $\alpha$ ] Define an ellipsoidal hull of the head model, which can be considered as a rough approximation to the head. Then also specify the region of hair pores on the ellipsoid.
- [ $\beta$ ] Calculate hair bending, based on a simplified simulation of a *cantilever beam*. This process also includes collision detection between each hair and the ellipsoid.
- [ $\gamma$ ] Cut hair and modify with slight adjustment, in order to get the desired shape in the final stage.

In step [ $\alpha$ ], the ellipsoid is employed simply for convenience in the design and calculation of hairstyle. For example, the pore positions are easily specified on the ellipsoidal hull, rather than on the original (polygonal) head model. This is because a polar coordinate system for the ellipsoid is available, which provides global guidance for explicit positioning. In addition, collision detection between the ellipsoid and hair is readily done at a low computational cost, compared to checking between the polygonal head model and hair. Though of course the "ellipsoidal" approximation is not accurate for general purposes, we believe that it is still valid and efficient for extracting the beauty of hair which is

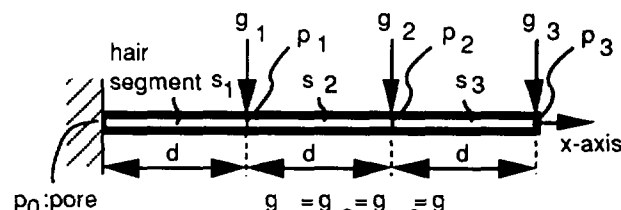
described in this paper.

The central idea of the modeling method is the use of a cantilever beam simulation for the hair bending calculation, which allows variations in hairdressing with volumetric and realistic appearance. The following sections are mainly devoted to describing the hair bending method.

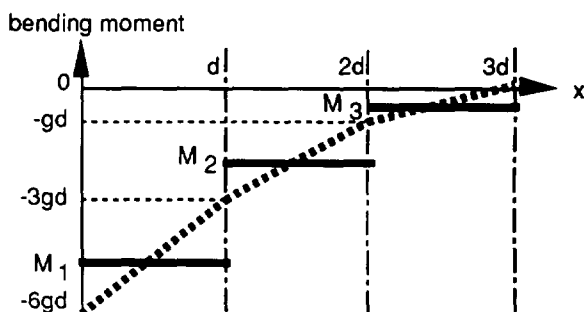
### 2.1 The cantilever beam simulation for hair bending

In the field of material strengths [10], the cantilever beam is originally defined as a straight beam with a one-sided and fixed support, as shown in Fig.1 (a). Let us employ the cantilever beam as our hair model, which is also shown later to give an efficient analogy for volumetric representation of hair.

The hairstyle modeling method then involves the process of hair bending, which is actually interpreted as the numerical simulation of the cantilever beam deformation. In order to describe the simulation technique, a two-dimensional case is first treated for simplicity. Suppose that the cantilever beam of two-dimensions in an initial state is set as shown in Fig. 1 (a), where one end of the beam is fixed. (This actually corresponds to the pore of a hair). Let us consider a typical case in which the beam is loaded by the external force  $\mathbf{g}$  uniformly distributed on the whole beam, such as gravity. Then two types of model deformation may occur: one is caused by bending moment and the other is by shearing force. The former deformation is principally activated, whereas the latter does not affect our purpose. Thus we just consider the bending momentum deformation. Let the  $x$ -axis be along the initial beam direction, and the  $y$ -axis be vertical to the direction. The  $y$ -axis indicates the deflectional direction, with the variable  $y$  representing deflection of the beam. Assuming that the model is elastically deformed, the following equation governs the



(a) Distribution loads of the cantilever beam for hair model



(b) Bending moment diagram

Fig. 1 Bending moment of the cantilever beam

deformation process:

$$\frac{d^2y}{dx^2} = -M/(E*I), \quad (1)$$

where  $E$  is Young's modulus, and  $I$  denotes the second momentum of area. The term  $E*I$  is usually referred to as the flexural rigidity, which depends on the beam material. Theoretically equation (1) does not hold in dealing with large deformation, but can be considered to be valid for our purpose of hairstyle modeling.

The calculation method of the above bending moment is illustrated in Fig. 1. Fast calculation is derived from the idea that the distributed load  $g$  is approximated by the finite sum of the *segmentally averaged* concentrated loads. For this idea, we suppose that the cantilever beam consists of finite linear segments with the same length. Let  $p_0, p_1, \dots, p_k$  be the node vectors of the segments, where  $p_0$  is the pore and  $p_k$  is the free end of the beam. In Fig. 1 (a), the beam consists of three segments  $s_0, s_1$ , and  $s_2$ , so that  $s_i$  corresponds to the vector  $p_{i-1}p_i$ , and the magnitude  $\|p_{i-1}p_i\|$  is equal to  $d$ , for  $1 \leq i \leq 3$ . Let  $g_0, g_1$ , and  $g_2$  be the copies of the force  $g$ , where each  $g_i$  is supposed to be a concentrated load at the node  $p_i$ . Then the bending moment at point  $x$  on the model would be represented by the graph of broken line in Fig. 1 (b). However, for simplicity, we assume the bending moment as being constant on each segment, as shown in Fig. 1 (b). The constant values  $M_i$  on the segment  $s_i$  are defined as:

$$M_i = -\|g\|d(\sum_{p=1}^{k-i} p + \sum_{p=1}^k p)^2/2 = -\|g\|d(k-i+1)^2/2. \quad (2)$$

The displacement  $y_i$  of the node  $p_i$  can be easily evaluated, using the following formula:

$$y_i = (-1/2)*(M_i/E*I)*d^2, \quad (3)$$

which is derived from equation (1). Suppose that  $p_{i-2}$  and  $p_{i-1}$  are known using formula (3). Then let us obtain the new position of the node  $p_i$ . To do so, get the vector  $e_i$  such that  $e_i$

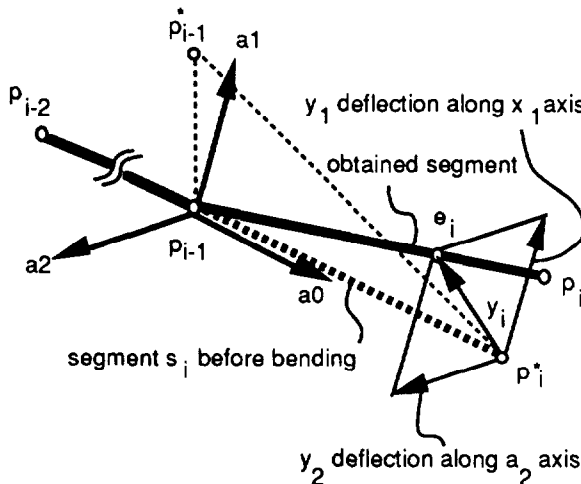


Fig. 2 Deflection of 3D hair model

$= p_{i-2}p_{i-1} + y_i$ , where the  $x$ -axis for the calculation is defined as being along the segment vector  $p_{i-2}p_{i-1}$  and the vector  $y_i$  is in the deflectional direction with its magnitude being equal to  $y_i$  in (3). The new node  $p_i$  is consequently defined as  $p_i = (d/\|e_i\|)e_i + p_{i-1}$ , satisfying  $\|p_{i-2}p_i\| = d$ . The vectors are successively obtained from  $p_1$  to  $p_k$ .

Let us now extend the calculation method to a three-dimensional case. First we introduce the coordinate system suitable for the method. The  $a_0$ -axis in Fig. 2 corresponds to the  $x$ -axis described above, that is, the  $a_0$  axis is defined as being along the segment vector  $p_{i-2}p_{i-1}$ . Let  $p^*_i$  be a point which is a distance  $d$  along the  $a_0$ -axis from  $p_{i-1}$ . Also  $p^*_{i-1}$  denotes a point which is far from  $p_{i-1}$  by a certain distance, so that the three points  $p_{i-1}, p^*_{i-1}$ , and  $p^*_i$  span a plane. Then the  $a_1$ -axis is defined as being vertical to the  $a_0$ -axis and on the plane. The  $a_2$ -axis is specified such that it is orthogonal to both axes. Now we apply the two-dimensional method to obtaining the deflections  $y_1$  along the  $a_1$ -axis and  $y_2$  along the  $a_2$ -axis, considering a respective component of the force. Supposing there is no compression of the beam, the desired deflectional vector  $y_i$  is obtained as  $y_1 a_1 + y_2 a_2$ , where the vectors  $a_1$  and  $a_2$  are from the orthonormal basis of the  $a_0-a_1-a_2$  coordinate system. Similar to the two-dimensional case, a new sequence of the beam nodes is obtained, using the deflectional vectors.

In applying the above cantilever beam simulation to hairstyle modeling, we should consider collision detection to prevent the hair model from intersecting the head or body. As is well

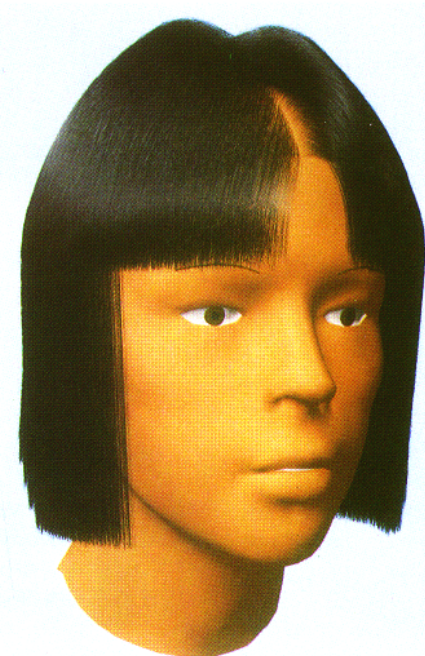


Fig. 3 Bobbed hair

known, the problem of collision detection is very difficult to solve in a general situation. The collision detection process in physically based modeling is generally rather time-consuming, compared to other calculation processes. Even if we concentrate only on collisions between the hair and the head, neglecting hair-hair collisions, it would still require a high computational cost. This is because it must be checked whether each segment of the hair intersects any polygon of the head, though in total the hair model typically consists of over 400,000 segments and the polygon head has about 10,000 polygons. So let us use the ellipsoidal approximation again. Then we avoid the hair model intersecting the ellipsoid in a very inexpensive way. The collision detection and avoidance are performed while obtaining the new sequence of the nodes  $p_i$ . Suppose that the two nodes  $p_{i-2}, p_{i-1}$  of the hair model are newly defined using the cantilever beam simulation and then modified to be out of the ellipsoid. Subsequently, it is easy to know whether the next node  $p_i$ , which is again the result of the beam simulation, is intersecting the ellipsoid. This is done by checking the signature of the quadric form  $E(p_i)$ , which defines the ellipsoid:  $E(p) = 0$ . If the node  $p_i$  is intersecting, then it is moved out in such a way that the resultant node is near the original point of  $p_i$  and it is on the plane spanned by the three points  $p_{i-2}, p_{i-1}$  and  $p_i$  (or an appropriate plane containing  $p_{i-2}$  and  $p_{i-1}$ , if these three vectors degenerate).

## 2.2 The modeling process and examples

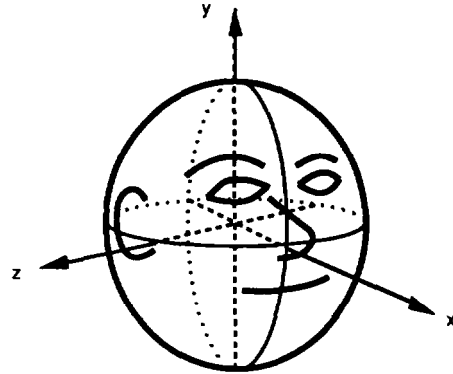
Though the hair bending process plays a central role in our hairstyle modeling, it just shows one physically faithful aspect of hair. Actually a hairdresser creates many artificial aspects, such as shearing, combing, tying up into a ponytail, etc. In this paper, relatively simple techniques are developed to model such artificial techniques to beautify hair. These are very naive and elementary, and they may become insufficient for achieving more accurate and realistic hairstyle modeling, but the sophisticated approaches for this have not been established yet to our knowledge.

Our modeling method is introduced through several examples. As a typical case, the modeling process of bobbed hair shown in Fig. 3 is described. First, the initial state is defined, as shown in Fig. 4 (a), where the pore positions and the initial length of hair are specified. Since there is no external force or gravity applied to the initial hair beams, they stand radially. By adding gravity, the hair beams go down, as illustrated in Fig. 4 (b). The hair near the top of the head is not deformed much, since the strands are essentially parallel to the gravity vector and the bending momentum is relatively small. The undulation of hair in front of the face is also observed in Fig. 4 (b), which is caused by the collision avoidance mentioned above. Then cutting, combing or brushing makes the hair more attractive in actual hairdressing. For the bobbed hair in Fig. 3, these kinds of techniques would give the short bangs, parting the hair at the middle of the head, and so on. Instead of using shears or a comb, cutting operations and bending calculations



(a)

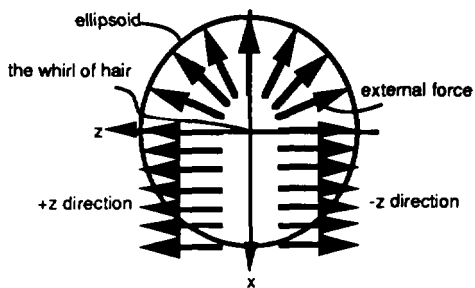
(b)



(c)

(d)

(a) Head positioning in the local coordinate system



(b) External force for the hairstyle in Fig. 3

Fig. 4 Hairdressing process

Fig. 5 Head coordinate system and examples of external force



**Fig. 6 Example hairstyles**

with additional external forces are used for the hairstyle modeling. In the cutting operations specification of the hair to be cut is performed using the polar coordinate system of the approximating ellipsoid and the threshold along the vertical direction, i.e. the  $y$ -axis direction shown in Fig. 5 (a). For instance the pore positions of the hair to be cut are specified by the range of the azimuth  $\phi$  and zenith angles  $\theta$  such as  $\phi_0 \leq \phi \leq \phi_1$  and  $\theta \leq \theta_0$ . Then the segments of the hair whose pores are in the range are not displayed if the  $y$  coordinate values of their nodes are less than the designated threshold. (In a rendering step, each hair is displayed as a polyline. For more details, see section 4). To comb the hair, some external forces in addition to gravity are selected. To illustrate this, suppose that the face indicates the positive  $x$  direction, and the  $y$ -axis is in the vertical direction, using the coordinate system shown in Fig. 5 (a). The external force field shown in Fig. 5 (b) is then applied to the hair segments that are located higher than the eyes. Fig. 4 (c) shows the result, in applying the cantilever beam simulation using force to the hair segments in the positive  $z$  region, where cutting is done during postprocessing. After this, the hair model in Fig. 4 (d) is obtained, by adding similar results for the hair in the negative  $z$  region. Again by shearing the back hair in Fig 4 (d), the hairstyle in Fig. 3 is consequently made, which illustrates well the efficiency of the method in representing a volumetric appearance of hair.

Fig. 6 illustrates some other hairdressing examples generated by our method. Fig. 6 (a) shows a hairstyle relatively similar to that of Fig. 3, while the drooping bangs and proper fluctuation of hair lengths are successfully produced. As for making the hairdo in Fig. 6 (b), the external force applied indicates the negative  $x$  direction, that is, from the face backwards. The tuft of hair at the side of the temple is also added. A tied hairstyle, or "ponytail" is represented in Fig. 6 (c), where the ponytail and other parts of the hair are individually designed. In making the short haircut in Fig. 6 (d), the cutting operation is somewhat elaborate as the number of hair segments not to be displayed is arranged depending on the height of the hair pore (i.e., the  $y$  value of the pore). These examples visually demonstrate the variety of realistic appearances achievable with the method.

### 3. Dynamical behavior of hair

An aesthetic feature in hair dynamics seems to appear typically in scenes where long hair is *gently* blowing in the wind or is swaying according to human movement, such as, running or looking back quickly. (Then the highlighted areas of the hair are also moving, which again fascinates us, but the rendering technique for this is described later). Considering these actual impressions of hair dynamics, the equation(s) to be employed here should at least control the *inertial* property of hair. In other words, some aesthetic features in hair animation are extracted by the method, which are obtained as the result of *inertia vs applied force*. To do so, simple ordinary differential equations are introduced in the following way.

In the previous section each hair strand is represented as a deformed beam, and is actually a collection of linked linear segments. For the purposes of animation, the hair model also has such a geometrical structure, whose segments may be considered to be rigid sticks this time. The proposed technique for pursuing dynamical behavior of hair is essentially reduced to solving the simple one-dimensional differential equation(s) of angular momentum for each hair. Then collision and interaction, such as a friction effect, of the hair strands with themselves and with the head are not rigorously considered. However, the technique gives a "roughly" approximate solution of these difficult problems. The solution simply means utilizing a pseudo-force field in solving the differential equations, beside rigorous treatments of applied forces and some other physical conditions. The pliability of hair is also described using a parameter for controlling the angles of adjacent segments of hair, which copes with the differential equations.

#### 3.1 One-dimensional projective equations for hair dynamics

Let us now consider the dynamics of a single hair, since hair self-interaction is not treated rigorously in the method. Then, taking the polar coordinate system as shown in Fig. 7, the behavior of the zenith angle  $\theta_i$  and the azimuth  $\phi_i$  of the  $i$ -th segment  $s_i$  of the hair are observed. Particular consideration is given to the shadows of the segment on the  $\Theta$  and  $\Phi$  planes

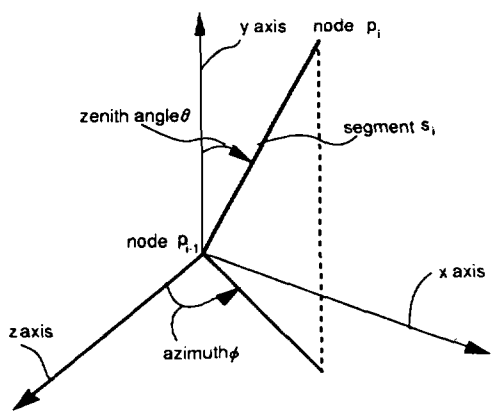


Fig. 7 The polar coordinate system for a hair segment

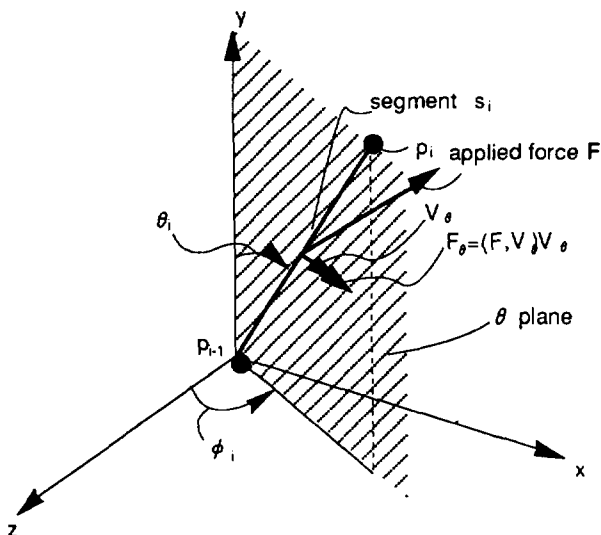


Fig. 8 Definitions of \$\theta\$ plane and \$F\_\theta\$

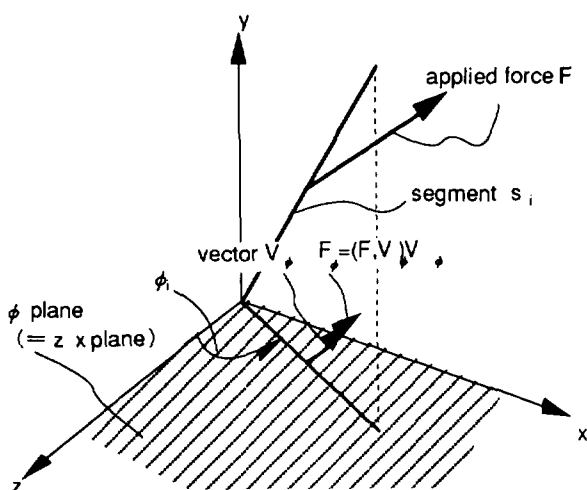


Fig. 9 Definitions of \$\phi\$ plane and \$F\_\phi\$

which are defined as shown in Figs. 8 and 9. The \$\theta\$ plane is the plane spanned by the y-axis and the segment \$s\_i\$. If \$s\_i\$ is almost parallel to the y-axis, then the \$\theta\$ plane is defined using the y-axis and an applied force \$F\$ instead of \$s\_i\$. The \$\phi\$ plane is defined as the \$zx\$ plane. Then, on these planes, the variables \$\theta\_i(t)\$ and \$\phi\_i(t)\$ with the time parameter \$t\$ may be governed by the ordinary differential equations:

$$\frac{d^2\theta_i}{dt^2} = c_i u_i F_\theta \quad (4)$$

$$\frac{d^2\phi_i}{dt^2} = c_i v_i F_\phi \quad (5)$$

where \$c\_i\$ corresponds to the reciprocal number of the inertia moment of \$s\_i\$;  
\$u\_i\$ is \$(1/2)\|s\_i\|\$;  
\$v\_i\$ is the half length of the segment that is the projection of \$s\_i\$ onto the \$\phi\$ plane; and  
\$F\_\theta, F\_\phi\$ are the “\$\theta, \phi\$ -components” of the applied force \$F\$ respectively, as shown in Figs. 8 and 9.

The above \$\theta\$ component \$F\_\theta\$ of the applied force field \$F\$ is the scalar value defined by \$F\_\theta = \|F\_\theta\| = (F, V\_\theta)\$, where \$V\_\theta\$ is the unit vector (i.e. the magnitude is equal to one) on the \$\theta\$ plane that is perpendicular to the segment \$s\_i\$. Similarly the \$\phi\$ component \$F\_\phi\$ is defined by \$F\_\phi = \|F\_\phi\| = (F, V\_\phi)\$, where \$V\_\phi\$ is the unit vector on the \$\phi\$ plane which is perpendicular to the projection segment of \$s\_i\$ onto the \$\phi\$ plane. Our idea is that we employ *one-dimensional projective equations* (4) and (5) for describing hair dynamics, though originally these govern *projective behaviors* of our hair model.

In the numerical simulation, these equations mean simple recurrence formulae of second order. Using the known values \$\theta\_i^{n-1}\$ and \$\theta\_i^n\$, the new value \$\theta\_i^{n+1}\$ at the time \$(n+1)\Delta t\$ is obtained by

$$\theta_i^{n+1} - 2\theta_i^n + \theta_i^{n-1} = (\Delta t)^2 c_i u_i F_\theta \quad (4)'$$

Similarly, from \$\phi\_i^{n-1}\$ and \$\phi\_i^n\$, the new value \$\phi\_i^{n+1}\$ is given by

$$\phi_i^{n+1} - 2\phi_i^n + \phi_i^{n-1} = (\Delta t)^2 c_i v_i F_\phi \quad (5)'$$

The calculation starts with the segment \$s\_1\$, and the new position of \$s\_i\$ is successively determined, using (4)' and (5)'. It should be noted that, in the calculation of (4)' and (5)', the discrete time loop concerning the parameter \$n\$ can be set as the inner loop while the outer loop is the segment number \$i\$. This would be useful for saving time in calculating many frames of a huge amount of hair. An example of the initial condition is that \$\theta\_i^0 = \theta\_i^{-1} = \theta\_i^{\text{init}}\$; \$\phi\_i^0 = \phi\_i^{-1} = \phi\_i^{\text{init}}\$, which means that the hair is still at the beginning. Other conditions for the parameters or input information about (4)' and (5)' are described next, which also involves rough treatment of collision

avoidance or self-interaction of hair.

### 3.2 Introducing a rough approximation of physics

#### 3.2.1 Inertia moment and its modification

Consider the straight stick  $S$  with length  $kd$  and line density  $\rho$ . Then its inertia moment  $I_S$  is given by  $I_S = (1/3)\rho(kd)^2$ . For our hair model, the terms  $c_i v_i$  and  $c_i u_i$  in (4) and (5) closely relate to this  $I_S$ . For example, suppose that the inertia moment  $I_i$  of  $s_i$  is proportional to  $1/i$  ( $1 \leq i \leq k$ ) and that  $I_k$  is equal to  $I_S$  (see [1] for a more mathematical treatment). Then  $I_i$  is given as  $I_i = (\rho/3i)k^3 d^2$ . The term  $(\Delta t)^2 c_i u_i$  in (4)' is consequently represented as  $(3(\Delta t)^2 i)/(2k^3 \rho d)$ . (For the term  $(\Delta t)^2 c_i v_i$  in (5)', a similar expression is obtained). This expression may be used for numerically estimating the magnitude of the righthand side of equation (4)'. In addition, it is noted that the kind of self-interaction effect can be described by arranging the  $c_i$ 's values. For example, if the  $c_i$ 's are selected as rather small for the segments near the top of the head, the hair near the top moves relatively slowly, when affected by an applied force field. This can be thought of as a "rough" approximation of the hair's frictional effect. Therefore in the method, the coefficients are appropriately arranged according to the situation.

Fig. 10 shows the four frames taken from a very short film representing a wind gust scene. The animation is made under the condition that  $\Delta t = 0.1$ ,  $d = \rho = 1.0$  and  $k = 18$ , where the number  $k$  is the maximum number of the segments used for the hair model shown in Fig. 10 (a). About 10,000 individual hairs are described for the scene. Then the applied force field  $F$  is defined as  $(-200, 0, 0)$  with the coordinate system in Fig. 5 (a). From the 16th frame,  $F$  is  $(-20, -250, 0)$ . The discontinuous change of the force field corresponds to the drastic change of an actual

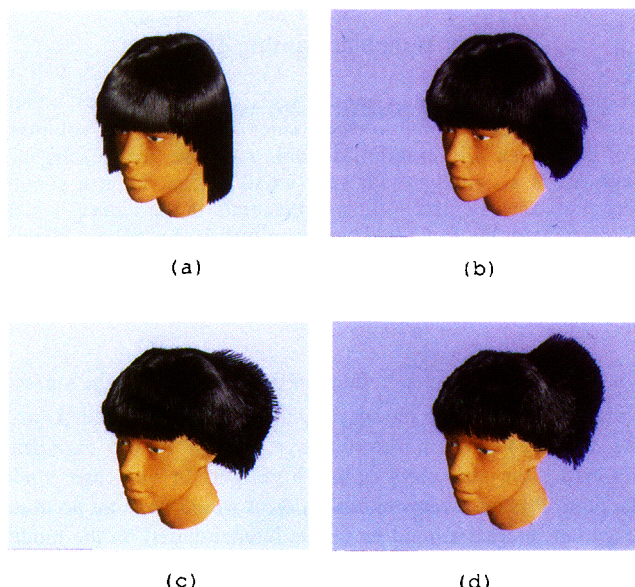


Fig. 10 A wind gust scene



(a)



(b)



(c)

Fig. 11 Example of dynamic collision avoidance

wind gust. The 10th frame is shown in Fig. 10 (b) and the 15th frame is in Fig. 10 (c). The hair undulation is observed in the 20th frame, as shown in Fig. 10 (d). This is caused by the drastic change of the wind vector field, which illustrates the effect of inertia vs applied force by the method. Note also that the bangs do not go through the forehead. This is achieved by using the pseudo-force field, which is described in the next section.

#### 3.2.2 Pseudo-force field

The method also provides a simple technique for avoiding in the mass hair collisions with the head. The technique implies introducing a pseudo-force field, instead of the specified force field. Let  $F$  be the force field specified by a user. In solving equations (4) and (5) for  $F$ , let us define the segment direction  $D_i$  of the hair segment  $s_i$ , using the ellipsoid equation  $E(p)$ :  $D_i = (E_x(p_i), E_y(p_i), E_z(p_i))$ , where  $E_x$ ,  $E_y$ , and  $E_z$  are partial derivatives of the algebraic polynomial. For a prescribed value  $\alpha$  ( $|\alpha| \leq 1$ ), it should be examined whether the inner product  $(D_i, F)$  is smaller than  $\alpha \|D_i\| \cdot \|F\|$ . If so, it means that the segment  $s_i$  is roughly in the opposite direction of  $F$ . In addition, if the segment is near the head model, then replace  $F$  by the pseudo-force  $\varepsilon_i F$ , where  $0 \leq \varepsilon_i \leq 1$ . The pseudo-force constants  $\varepsilon_i$  for the segments near a pore are usually assigned smaller values, whereas those for the segments near the endpoint  $p_k$  are equal to 1. The pseudo-force  $\varepsilon_i F$  near the pore can be understood as the simplification of the composite force of  $F$  and the repulsive force.

An applied example of the pseudo-force field is found in Fig. 11. The initial state with  $F = 0$  is shown in Fig. 11 (a).

The result without the pseudo-force effect, which means all  $\epsilon_i$  are set at 1.0, is shown in Fig. 11 (b), where many hairs on the left side go through the head by the force  $F = (0, 0, -500)$ . Fig. 11 (c) shows the pseudo-force effect, where  $\alpha = -0.75$  and the coefficients  $\epsilon_i$  of the segments near the head are assigned 0.1.

### 3.2.3 Joint angle adjustment controlling stiffness

For our hair model, the joint angle  $\vartheta_i$  at the node  $p_i$  is the angle between  $\vec{p_i p_{i-1}}$  and  $\vec{p_i p_{i+1}}$ . Then the stiffness of the hair model is prescribed by the parameters  $\sigma_i$  ( $0^\circ \leq \sigma_i \leq 180^\circ$ ). The  $i$ -th stiffness parameter  $\sigma_i$  works after the new  $p_{i+1}$  is determined using the recurrence formulae (4)' and (5)'. If  $\vartheta_i$  is greater than  $\sigma_i$ , the node  $p_{i+1}$  is then adjusted such that the joint angle is equal to  $\sigma_i$ . Usually the stiffness parameters whose nodes are near a pore are set at  $180^\circ$  (that is, no adjustments of the nodes are done). And, in describing a smoother curve of hair, the parameters  $\sigma_i$  would be rather small, such as  $10^\circ$  or  $15^\circ$ , for the nodes far from a pore.

A typical application of this technique is the description of gently blowing hair with locally subtle fluctuations, as shown in Fig. 12. In this case each hair strand fluctuates according to the given uniform random numbers, after obtaining the new node positions by (4)' and (5)'. The use of the random numbers is made not for each frame, but for one per ten frames, to avoid excess fluctuations. Then, using the stiffness parameters, the obtained hair strand is rearranged in order to maintain the curve's smoothness. The local fluctuations are caused by the short haircut and the drastic change of the force field (similar to the case of Fig. 10). In Fig. 12 (a), the fluctuations are not observed clearly, since the stiffness parameters are set at  $180^\circ$ . On the other hand, if the parameters  $\sigma_i$  are set rather small as described above, then the fluctuations are exaggerated while preserving the hair's smoothness, as described in Fig. 12 (b). The efficiency of the stiffness parameters is obvious, but a careful choice of the parameters' values is currently required to obtain a desired result.



Fig. 12 Effect of joint angle control

## 4. Rendering technique and numerical results

### 4.1 Anisotropic reflection model for a three-dimensional curve

The rendering method are rather restrictive for fast processing, whereas the main contribution of this paper is toward modeling and animating hair. In particular shadowing effect is disregarded. As stated in the introduction, alternative rendering techniques [5, 8] would be helpful for more accurate description of hair.

The color of the hair treated in this paper is relatively dark brown or black, which allows the simplified rendering model described here still to be powerful. At the rendering stage the geometry of our hair model is represented as a collection of three-dimensional curves, which consequently consists of the polylines. Let us now consider a standard illumination equation involving ambient, diffuse and specular components. In order to describe glossy hair, the specular component seems to be dominant among the three components, whereas the diffuse term is neglected for simplicity. The resulting intensity of hair is supposed to be the sum of the ambient constant and specular component.

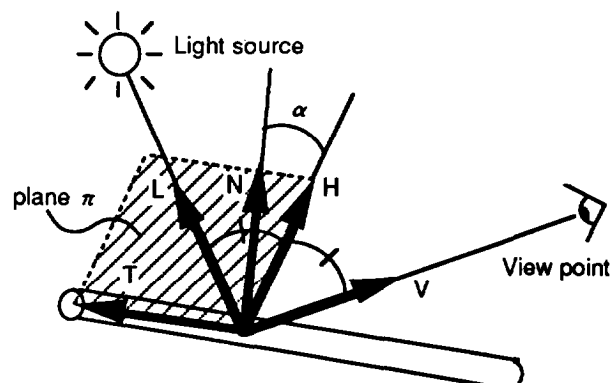


Fig. 13 Specular lighting geometry

Mathematically the hair model consists of polylines which have ill-defined normal vectors, since they have no volumes. To derive an illumination model, suppose that each hair segment is a cylinder with very small radius. Then a simple technique for calculating the specular term is introduced, which is motivated by Fig. 13. The technique is based on Blinn's specular model [2], that is, the specular term  $\Phi_s$  at the point P on a surface is defined by:

$$\Phi_s = k_s (N, H)^n \quad (6)$$

where  $k_s$  is the specular reflection coefficient,  $N$  is the surface normal at P,  $H$  is the halfway vector of the light vector  $L$  and the vector  $V$  pointing to the eye, and  $n$  is the exponent indicating the sharpness of the highlight. In our case, since the point P is on a very thin cylinder, it would be more accurate to get an integral around its circumference based on the model (6). However, the specular component proposed here is represented as the above  $\Phi_s$  in (6), taking the normal  $N$  on the plane  $\pi$  spanned by the vector  $H$  and the cylinder's tangent  $T$ .

Then, as shown in Fig.13, the term  $(\mathbf{N}, \mathbf{H})$  in (6) is easily evaluated using the known vectors:

$$(\mathbf{N}, \mathbf{H}) = \cos \alpha = 1 - (\mathbf{T}, \mathbf{H})^2 \quad (7)$$

Another algebraic proof of (7) is again easy to see. Since the vectors  $\mathbf{N}$  and  $\mathbf{T}$  constitute the orthonormal basis of the plane  $\pi$ , the following vector expression is obtained :  $\mathbf{H} = (\mathbf{N}, \mathbf{H})\mathbf{N} + (\mathbf{T}, \mathbf{H})\mathbf{T}$ . Then, by taking an inner product on both sides, the scalar relation holds:  $1 = (\mathbf{N}, \mathbf{H})^2 + (\mathbf{T}, \mathbf{H})^2$ , which leads us to equation (7). Thus the resultant specular term at  $\mathbf{P}$  is defined as

$$\Phi_s(\mathbf{P}) = k_s \{1 - (\mathbf{T}, \mathbf{H})^2\}^{n/2}. \quad (8)$$

The expression simply means that the actual highlight intensity is approximated by the strongest one in varying the surface normal at  $\mathbf{P}$ . This also gives an alternative formulation of the specular distribution based on Phong's model [4], but produces different effects in general [3].

The total intensity at a point  $\mathbf{P}$  on a cylinder is consequently given as

$$I(\mathbf{P}) = I_a k_a + I_s \Phi_s(\mathbf{P}), \quad (9)$$

where  $I_a$  is the intensity of the ambient light,  $k_a$  is the ambient reflection coefficient,  $I_s$  is the intensity of the light source and  $\Phi_s(\mathbf{P})$  is of the form in (8). In rendering the hair model, the ambient reflection coefficient  $k_a$  also plays an important role.

The coefficient  $k_a$  is a material property, so that it should be distinguished in rendering each hair, since the actual ambient color of hair is usually heterogeneous. In our situation, introducing a normal distribution,  $k_a$  fluctuates so randomly that it takes the same value on each hair strand, but differs between strands. The qualities of the resultant images derived from these simplifications are illustrated in Figs. 3-6, where anisotropy of hair reflection is observed, for example, like a halo. The quantitative effect for fast processing is demonstrated in the next section.

#### 4.2 Rasterization process and computational costs

The z-buffer algorithm is now available as a hardware facility of current graphics workstations. The above rendering algorithm can be combined with the hardware benefit in the rasterization process. Let us suppose that the width of the hair segment on the screen is a multiple of the pixel size. As described before, let  $\mathbf{p}_0, \mathbf{p}_1, \dots, \mathbf{p}_k$  be the nodes of the hair segments  $s_1, s_2, \dots, s_k$ . The color of the nodes is first defined by  $I(\mathbf{p}_i)$  in equation (9), where the tangent vector  $\mathbf{T}$  is defined as  $\overrightarrow{\mathbf{p}_{i-1}\mathbf{p}_i} / \| \overrightarrow{\mathbf{p}_{i-1}\mathbf{p}_i} \|$ . Then the color at each point on the segment is linearly interpolated by the hardware support. Thus the z-buffer algorithm can deal with the hair



**Fig. 14 Blowing in the wind**

segments, along with polygon data. It should also be noted that the technique can be extended to the case where the hair width in the obtained image is less than the pixel size. This is easily achieved by a oversampling technique. In Fig. 14, about 50,000 hair strands are described whose width is 1/4 pixel size and the image resolution is 1024×783.

The presented method for modeling, rendering and animating of hair is implemented on a Silicon Graphics Iris Power Series workstation with a VGX graphics board. The provided hardware supports involves the z-buffer algorithm, anti-aliasing and linear color interpolation. Typically the generated model has about 20,000 hairs, each of which is at most 20 linear segments. The wall clock time for the hairstyle modeling (mainly for the hair bending calculation) was about 50 seconds, whereas it averaged around 40 seconds per frame in the animation calculation. As for a rendering time, it was usually several seconds. In particular, the image with a different camera angle was obtained in almost real time. Even in adding the anti-aliasing process, it took less than 15 seconds on average at 1024 × 1024 pixels resolution.

Finally we note that the fast processing facilities of the method allow quick feedback in previewing. In particular, an animation preview is easily done under the condition that the number of hairs is less than a few hundred. Then hair segment data generation by the method for making an animation takes less than 2 seconds per frame. Consequently, after stacking the hair data for hundreds of frames, the near real time animation preview is performed by the fast rendering method. The projective equations allow numerically stable simulations, so that longer animations can be produced than those illustrated in this paper. However interactive facilities would be desired for explicit specification of the external forces in pursuing more complex hair dynamics.

## 5. Concluding remarks

This paper has presented a simple method for describing human hair, which is essentially a combination of simple ordinary differential equations and some intuitive heuristics. The obtained images have demonstrated well the efficiency of the method. It should then be noted that these differential equations are directly combined with the aesthetic observations, sacrificing rigorous formulation of physics. Moreover this allows to easily introduce fast processing and several efficient heuristics to the method, which is evident in particular for hair dynamics. The one-dimensional projective equations are solved under a pseudo-force field. Consequently the method provides a big advantage over existing approaches, in fast processing and descriptive power of hair's natural beauty. We are currently working on extending the method, giving "rough" approximate solutions of the problems in collision detection between hair and a human body or other objects, in order to deal with the long hair in a more general situation.

The available range of the proposed method may still be small, compared to the diversity and variety of actual human hair. It is also understood that several assumptions used for the method do not hold in general. Nevertheless we feel the method is valuable as a first trial for extracting some aesthetic features of hairstyle modeling and animation of hair dynamics.

## Acknowledgements

The authors would like to thank Ryozo Takeuchi, George Nishiyama, Akio Yajima and Masao Yanaka for their continuous encouragement and support. Thanks to Munetoshi Unuma, Kiyoshi Arai and Hiroaki Takatsuki for helpful discussions. The first author thanks Takeshi Sato for his programming support. The authors also wish to thank Dr. Carol Kikuchi for proofreading and suggestions.

## Reference

- [1] Arnold V. I. *Mathematical Methods of Classical Mechanics* (2nd ed.) Springer Verlag New York, 1989
- [2] Blinn J. Models of Light Reflection for Computer Synthesized Pictures *Computer Graphics* 11, 3 (July 1977) 192 -198.
- [3] Foley J., van Dam A., Feiner S. and Hughes J. *Computer Graphics: Principles and Practice*, Addison-Wesley, 1990.
- [4] Kajiya J. T. and Kay T. L. Rendering Fur with Three Dimensional Textures *Computer Graphics* 23, 3 (July 1989) 271 -280.
- [5] LeBlanc A. M., Turner R., and Thalmann D. Rendering Hair using Pixel Blending and Shadow Buffers *The Journal of Visualization and Computer Animation* 2, 3 (1991) 92-97.
- [6] Magnenat-Thalmann N. and Thalmann D. Complex Models for Animating Synthetic Actors *IEEE Computer Graphics and Applications* 11, 5 (September 1991) 32-44.
- [7] Miller, Gavin. S. P. From Wire-Frame to Furry Animals *Proceedings of Graphics Interface '88* (October 1988) 138-146.
- [8] Rosenblum, R. E., Carlson, W. E. and Tripp, III, E. Simulating the Structure and Dynamics of Human Hair: Modelling, Rendering and Animation. *The Journal of Visualization and Computer Animation* 2, 4 (October-December 1991), 141-148.
- [9] Terzopoulos D. and Fleischer K. Deformable Models *The Visual Computer* 4, 6 (December 1988) : 306 -331.
- [10] Timonshenko S. *Strength of Materials : Part I Elementary Theory and Problems* D. Van Nostrand Company, Princeton, New Jersey, 1955
- [11] Watanabe, Y. and Suenaga, Y. A Trigonal Prism-Based Method for Hair Image Generation *IEEE Computer Graphics and Applications* 12, 1 (January 1992), 47-53.